

PHYSICAL REVIEW B

CONDENSED MATTER

THIRD SERIES, VOLUME 26, NUMBER 2

15 JULY 1982

Amorphous-nonmetal—to—crystalline-metal transition in electrochromic iridium oxide films

S. Hackwood, A. H. Dayem, and G. Beni

Bell Laboratories, Holmdel, New Jersey 07733

(Received 17 August 1981)

We report studies of sputtered iridium oxide films (SIROF's) by differential thermal analysis, evolved-gas analysis, scanning electron microscopy, x-ray diffraction, and electrical-conductivity measurements. SIROF's undergo an irreversible exothermic transition at $\sim 300^\circ\text{C}$ with ~ 1 eV energy release and no associated decomposition. There is a second endothermic transition at $\sim 700^\circ\text{C}$, which is associated with dehydration. We show that the first transition is an amorphous-to-crystalline transition. The amorphous state is nonmetallic, whereas metallic conductivity is observed in the crystalline state. After undergoing the transition, SIROF's lose their good electrochromic and electrocatalytic properties. We show that these properties are associated with the fast-ion mobility in the amorphous state.

I. INTRODUCTION

Sputtered iridium oxide films (SIROF's) have unusual electrocatalytic^{1,2} and electrochromic³⁻⁷ properties. As electrocatalysts, they are highly efficient anodes for water electrolysis, since they have a low overvoltage for oxygen evolution. Ruthenium and iridium oxides have the lowest overvoltage for oxygen evolution of all the platinum metals. In an acidic solution ($0.5M$ H_2SO_4) SIROF's are stable² at potentials greater than 1.85 V [versus reversible hydrogen electrode (RHE)] where other catalysts, such as ruthenium oxide, corrode⁸ at a significant rate. SIROF's also exhibit efficient electrocatalytic properties for bromine evolution. For example, a solar-cell-electrolytic system⁹ (under development at Texas Instruments) employs silicon *p-i-n* junctions coated with¹⁰ SIROF's for the anodic evolution of Br_2 from a HBr electrolyte.

SIROF's also show electrochromic behavior and are promising materials for displays.¹¹ Electrochromism is a persistent but reversible color change induced by an electrochemical reaction. Several ion-insertion compounds (e.g., WO_3 , MoO_3 , V_2O_5) exhibit electrochromism.¹² Their optical properties change markedly as the number of in-

serted ions (e.g., H^+ , Li^+ , Na^+) increases or decreases. For example,¹³ evaporated films of WO_3 change from transparent to blue upon insertion of protons (and simultaneous insertion of electrons for charge neutrality).

SIROF's are electrochromic ion-insertion materials. Although the exact mechanism of ion insertion is not yet known, SIROF's have received considerable attention since their electrochromic properties are attractive³⁻⁶ from a technological point of view. These films exhibit good contrast (transparent to black) upon insertion of ~ 20 mC/cm² of charge. They have fast response times (color changes occur within ~ 50 msec) and memory (coloration persists for many hours after the ion-insertion process has taken place and the cell is open-circuited). In addition, owing to fast ion transport within the films, their temperature range of operability¹⁴ is wider than that for other electrochromic materials. Their most remarkable properties, however, are their stability and absence of corrosion in a wide variety of electrolytes.

From preparation,⁴ it is known that these materials are hydrated oxides of iridium, but the ratio of components (Ir, O_2 , and H_2O) is not known exactly. On the other hand, the stoichiometry and structure is crucial to the film's properties, since

compositionally similar compounds do not exhibit the same properties. For example, crystalline IrO_2 with a rutile structure is not electrochromic¹⁵ and does not have exceptional electrocatalytic properties.^{16,17} Anodically grown films of iridium oxide¹⁸ exhibit electrochromism, but have poor stability in most electrolytes. Only in *ad hoc* electrolytes (e.g., pH 3.5 Na_2SO_4) has a cycle lifetime larger than 10^6 cycles been reported.¹⁹ During oxygen evolution, anodic films initially exhibit current densities as high as those for SIROF's, but the rate of corrosion is so fast that after a few minutes they are dissolved.²⁰ Thus the SIROF's stoichiometry and/or bonding structure must be significantly different from those of anodically grown films and bulk iridium oxide.

In this paper, we have investigated the film structure and composition of SIROF's and phases by differential thermal analysis (DTA), evolved gas analysis (EGA), scanning electron microscopy (SEM), x-ray diffraction, and four-probe conductivity measurements. We have found that SIROF's undergo an irreversible exothermic transition at $\sim 300^\circ\text{C}$ with ~ 1 eV energy release and no associated decomposition. There is a second endothermic transition at $\sim 700^\circ\text{C}$ that is associated with dehydration. We have identified the first transition as an amorphous-to-crystalline transition. The amorphous state is nonmetallic, whereas metallic conductivity is observed in the crystalline state. In the crystalline-metallic state the SIROF's lose their good electrochromic and electrocatalytic properties. We show that these properties are associated with the fast ion mobility in the amorphous structure.

In Sec. II, we present the results of DTA, EGA, and x-ray diffraction, which provide clear evidence for the amorphous-to-crystalline transition. In Sec. III, we report the electrocatalytic and the electrochromic properties of the new phase (polycrystalline) obtained upon heating above $\sim 300^\circ\text{C}$. In Sec. IV, we report conductivity measurements from 3 to 1000 K. The magnitude of the conductivity does not vary considerably over this range of temperature, but the temperature dependence identifies the amorphous and crystalline phases as nonmetallic and metallic, respectively.

II. AMORPHOUS TO CRYSTALLINE TRANSITION

In this section, we report and discuss DTA, EGA, SEM, and x-ray diffraction measurements.

A. Experimental

We prepared the SIROF's as described in Ref. 4. Sputtering time was approximately 4 h. We used two substrates for each deposition: a quartz substrate and a gold-leaf substrate. The first substrate provided films with well-defined sharp edges along their lengths; the latter provided samples easily weighed for use in DTA and EGA. Thicknesses were measured using an α -step stylus instrument of $\pm 0.01\text{-}\mu\text{m}$ accuracy. The gold substrates ($3\text{ cm}^2 \times 10\text{ }\mu\text{m}$) were weighed before and after deposition on a microbalance of $\pm 1\text{-}\mu\text{g}$ accuracy.

DTA was performed from 25 to 1000°C using a Mettler 2000 instrument with alumina as the reference material at a scan rate of $10^\circ\text{C}/\text{min}$. The DTA chamber was purged with argon at a flow rate of $100\text{ cm}^3/\text{min}$. For each sample examined by DTA, we examined a similar sample by EGA (Ref. 21) to detect loss of H_2O , O_2 , H_2 , or Ar at a vacuum of 10^{-2} Torr and at the same scan rate as that for DTA. SIROF's deposited on sapphire substrates were examined before and after the phase transition by x-ray diffractometry using an incident angle of 4° and by scanning electron microscopy. The x-ray data presented are corrected for an air-scattering component.

B. Results

The sample thickness of as-deposited SIROF's is $\sim 3000\text{ \AA}$. The density of as-deposited SIROF is $\sim 10.0\text{ g/cm}^3$, whereas bulk IrO_2 has a density $\sim 11.68\text{ g/cm}^3$. After electrochromic or electrocatalytic operation in aqueous electrolytes the SIROF's density decreases to 7.8 g/cm^3 owing to water uptake.⁷ SEM shows no feature above $0.05\text{ }\mu\text{m}$.

Figure 1 shows the results of DTA and EGA measurements. The DTA curve [Fig. 1(a)] shows a large exothermic peak at $\sim 300^\circ\text{C}$ and a small broad endotherm at $\sim 700^\circ\text{C}$. Both transitions are irreversible.

We estimated the change in enthalpy ΔH of the exothermic peak (at $\sim 300^\circ\text{C}$) from the area of the DTA curve (calibrated against the melting point of lead at 327°C). We found $\Delta H \sim 1.1\text{ eV}$. Substrate effects were eliminated, as similar results were obtained for SIROF's deposited on aluminum and mica.

The EGA [Fig. 1(b)] shows the relative intensity of emitted gases during heating. The small amount of argon incorporated during the deposi-

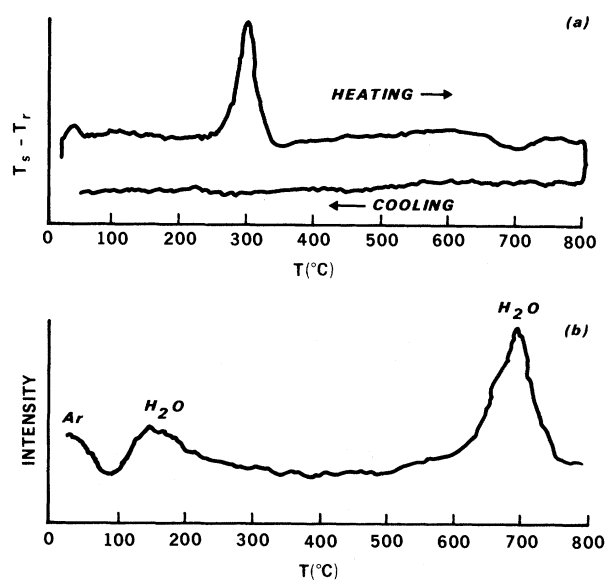


FIG. 1. (a) Differential thermal analysis and (b) evolved gas analysis for SIROF's on gold. T_s and T_r refer to sample and reference temperature, respectively. (a) shows a large exotherm at $\sim 300^\circ\text{C}$ and a small endotherm at $\sim 700^\circ\text{C}$. Both transitions are irreversible. (b) refers to the heating cycle only. The peaks showing H_2O emission are also accompanied by H_2 and O_2 evolution.

tion process is emitted at $\sim 30^\circ\text{C}$; some hydrogen, oxygen, and water are lost at $\sim 120^\circ\text{C}$ and a large amount at $\sim 700^\circ\text{C}$.

Figure 2 shows the results of x-ray diffraction analysis. Figure 2(a) shows the diffraction trace for an as-deposited film at room temperature. There is no evidence of order. Order begins to appear upon heating above $\sim 300^\circ\text{C}$. Figure 2(b) shows the diffraction pattern after annealing these samples at 590°C . The three clearly identifiable peaks correspond to the IrO_2 rutile structure as shown by comparison with Fig. 2(d). The size of the crystalline grains formed after the annealing is $\sim 150 \text{ \AA}$. Upon further heating to 790°C the size of the crystalline grains increases to $\sim 250 \text{ \AA}$. As is evident from Fig. 2(c) the film now has the same diffraction pattern as IrO_2 . The transition is irreversible. Upon cooling, the diffraction patterns remain unchanged [i.e., as in Fig. 2(c)], in agreement with the irreversibility of the DTA data. The SEM data once again did not show any features above $0.05 \mu\text{m}$.

C. Analysis

From the DTA, EGA, SEM, and x-ray data we can draw the following conclusions.

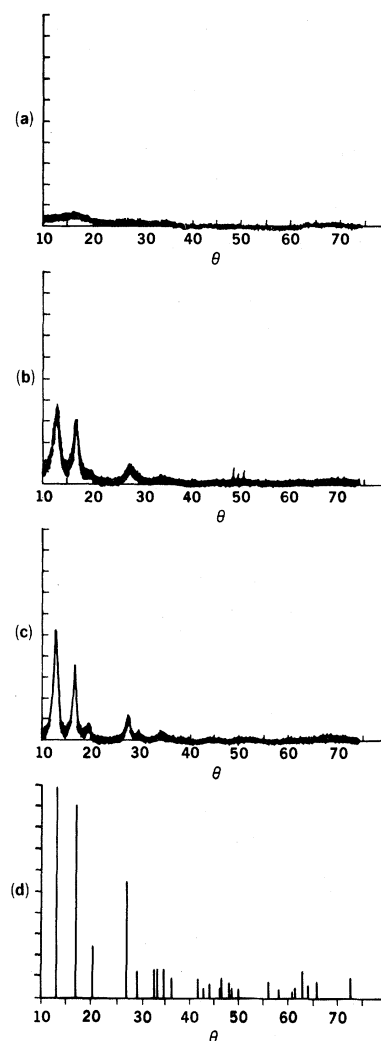


FIG. 2. X-ray diffraction analysis. (a) shows the results of an x-ray diffraction for an as-deposited film at room temperature. (b) and (c) show the x-ray diffraction data taken after annealing these samples at 590 and 790°C , respectively. The three clearly identifiable peaks correspond to the IrO_2 rutile structure as shown by comparison with (d).

(1) As-deposited SIROF's contain (beside traces of trapped argon) some water, even though they are prepared in nominally dry atmosphere. Water vapor is almost impossible to eliminate from the sputtering apparatus, so our findings are not surprising. Some of this water is lost upon heating in vacuum at $\sim 120^\circ\text{C}$.

(2) A large enthalpy change, $\Delta H \sim 1.1 \text{ eV}$, at $\sim 300^\circ\text{C}$ suggests a rearrangement reaction involving a change in bonding. No change in stoichiometry appears to take place, since EGA shows no gas evolution. Furthermore, the inert ar-

gon atmosphere precludes oxidation by atmospheric oxygen. The x-ray data show clearly that the enthalpy change is due to an amorphous-to-crystalline transition. The increase of crystalline grain size upon additional heating above the transition temperature is not associated with any large release of energy, as shown by DTA.

(3) The endothermic process at $\sim 700^\circ\text{C}$ is a dehydration associated with a further loss of water, H_2 , and O_2 . This is supported by the fact that a likely stoichiometry of the SIROF's is $\text{IrO}_2 \cdot 2\text{H}_2\text{O}$ [see Eq. (2) below]. This form of hydrated iridium oxide is known²² to dehydrate at $\sim 760^\circ\text{C}$.

III. PROPERTIES OF POLYCRYSTALLINE SIROF's

The polycrystalline phase of SIROF's obtained upon heating above $\sim 300^\circ\text{C}$, in contrast with the amorphous phase, has poor electrocatalytic and electrochromic properties.

A. Electrocatalysis

The electrocatalytic activity was determined for amorphous and polycrystalline SIROF's deposited on tantalum substrates as described in Ref. 2. The current density measured at a given voltage (under potentiostatic control) for the oxygen evolution reaction in $0.5M$ H_2SO_4 electrolyte is taken to be a measure of the catalytic activity. The current density at 1.6 V [versus a saturated calomel electrode (SCE)] decreases by a factor of ~ 6 for polycrystalline SIROF's.

B. Electrochromism

The electrochromic properties of the polycrystalline SIROF's were also examined in $0.5M$ H_2SO_4 electrolyte. The current-voltage characteristics of the SIROF's on sapphire substrates were examined in the potential range 0.0 – 1.0 V (versus SCE). The cyclic voltammogram recorded at a sweep rate of 2 mV/sec is shown in Fig. 3(a) for both amorphous (solid curve) and polycrystalline (dashed curve) samples.²³ At this slow sweep rate the system is in quasiequilibrium, i.e., the voltammogram is not distorted by resistivity effects, and thus it measures accurately the thermodynamics of ion insertion. Since amorphous SIROF's are ion-insertion materials and the voltammogram in the range 0 – 1 V (SCE) shows complete reversibility, a charge capacity ΔQ can be defined as the charge

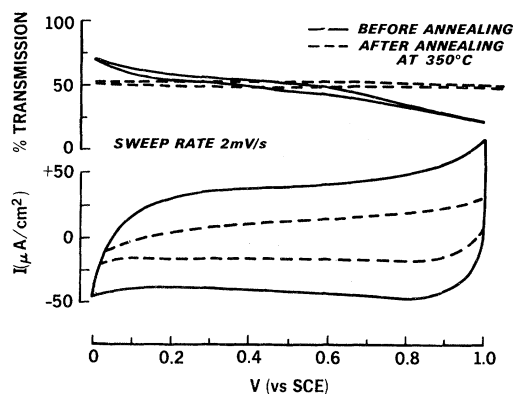


FIG. 3. (a) Cyclic voltammogram recorded at a sweep rate of 2 mV/sec for both amorphous (solid curve) and polycrystalline (dashed curve) samples. (b) Transmission of light (633 nm monitored with a He-Ne laser) through amorphous (solid curve) and polycrystalline (dashed curve) SIROF's.

inserted when the potential is stepped between two arbitrarily chosen limits. ΔQ is related to the film thickness and the number of accessible Ir sites.^{4,14} For SIROF's over the potential range 0 – 1 V (SCE) the number of accessible sites is ~ 0.7 per Ir atom.

As shown in Fig. 3(a), the charge inserted in cycling the crystalline film is about one third of the charge inserted in cycling the amorphous film ($\Delta Q \sim 20$ mC/cm² for the amorphous films and $\Delta Q \sim 8$ mC/cm² for the polycrystalline films). Thus, the number of "color centers" created by the ion-insertion process is substantially reduced in the crystalline state, although the reason for this is not yet understood. This is evident from Fig. 3(b), which shows the light transmission (at 633 nm from a He-Ne laser monitored by a Si photodiode) through amorphous (solid curve) and polycrystalline (dashed curve) SIROF's. The electrochromic effect is not detectable in the polycrystalline sample.

C. Analysis

Thus both the electrocatalytic and electrochromic properties of amorphous SIROF's deteriorate substantially after the film goes through the amorphous-to-crystalline transition at $\sim 300^\circ\text{C}$. Clearly, structure plays an important role.

Ion-insertion materials are mixed conductors, i.e., ionic and electronic conductors. For fast electrochromic response, both ionic and electronic conductivities must be high. If one of the two con-

ductivities is substantially reduced, properties that depend on fast ion insertion and transport will be affected. It is likely that upon undergoing the structural transition from amorphous to crystalline, the ionic and/or electronic conductivities are reduced so that a poor electrochromic and electrocatalytic material results. We have, therefore, investigated the SIROF's electronic conductivity, as discussed in the next section.

IV. NONMETAL-METAL TRANSITION

In this section we report and analyze electronic conductivity measurements in the temperature range 2–1000 K.

A. Experimental

SIROF's were deposited on sapphire substrates up to a thickness of $\sim 3000 \text{ \AA}$. The electrical conductivity was measured by a four-probe method using gold-plated pressure contacts held onto the SIROF surface by ceramic spacers. A current of $200 \mu\text{A}$ was allowed to flow between the two outside probes. Conductivity was measured in air from 298 to 1000 K and in a helium atmosphere 298 to 2 K.

B. Results

Figure 4 shows the temperature dependence of as-deposited SIROF's from room temperature to $\sim 750^\circ\text{C}$. In the upper curve, the resistivity is measured upon heating, and in the lower curve,

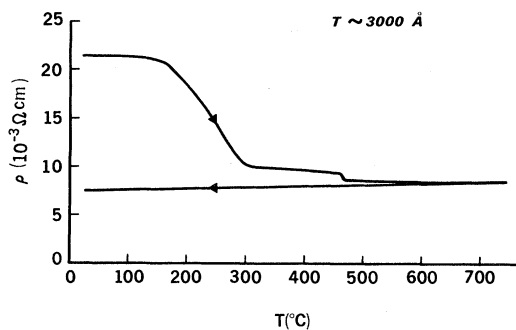


FIG. 4. Temperature dependence of as-deposited SIROF's from room temperature to $\sim 750^\circ\text{C}$. In the upper curve, the resistivity is measured upon heating, and in the lower curve, upon cooling.

upon cooling. The figure shows that the various events encountered in the DTA, EGA, and x-ray measurements are also present in the resistivity measurements. Specifically, water emission around $\sim 120^\circ\text{C}$ corresponds to the first decrease of resistivity; the second decrease occurs around $\sim 300^\circ\text{C}$. This is the temperature of the amorphous-to-crystalline transition.

The drop in resistance during the amorphous-to-polycrystalline transition is disappointingly small, as is the drop in resistivity when the sample cools back to room temperature. We have thus investigated in more detail the nature of the electronic conduction by measuring the resistivity at low temperature. The results are shown in Fig. 5. Before annealing, the sample behaves like a highly doped semiconductor, since the resistivity rises slowly with decreasing temperature and reaches a value 1.25 times the room temperature value at 2 K. After annealing, the resistivity decreases with temperature, indicating metallic behavior. However, the decrease in resistance is very small. The residual resistance at 2 K is approximately equal to its value at room temperature. Thus, in spite of its rutile phase, the material must contain a large number of impurities and crystalline defects that dominate its conductivity mechanism even at room temperature.

C. Analysis

The small difference in magnitude of the resistivity between amorphous and crystalline phases shows that although a nonmetal-to-metal transition

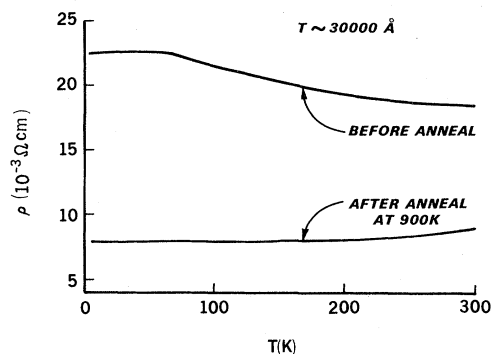


FIG. 5. Resistivity at low temperature. Before annealing the sample behaves like a highly doped semiconductor, since the resistivity rises slowly with decreasing temperature and reaches a value 1.25 times the room temperature value at 2 K. After annealing at 300 K, the resistivity decreases with temperature indicating metallic behavior. However, the decrease in resistance is very small.

takes place, SIROF's are far from purely stoichiometric materials. This is not surprising, since during reactive sputtering no measures were taken to ensure that the deposited films have the required 1:2 stoichiometry necessary to produce IrO_2 . The film is most likely composed of a mixture of Ir, O, IrO_2 , H_2O , and $\text{Ir}(\text{OH})_3$. From the x-ray data IrO_2 is the major component. The remaining components act as impurities, which together with crystalline defects and grain boundaries prevent the conductivity from reaching the metallic values of IrO_2 , which is $\rho \sim 5 \times 10^{-5} \Omega^{-1} \text{cm}^{-1}$ along the c axis.²⁴

More importantly, the small variation of resistivity in the ordered and disordered phases shows clearly that the deterioration of the electrochromic and electrocatalytic properties is not due to a decrease of the electronic conductivity in the polycrystalline phase. Therefore it is likely that the ionic conductivity decreases significantly in going from the amorphous to the polycrystalline phase.

V. DISCUSSION

In other electrochromic materials it has been recognized¹³ for some time that structure plays an essential role in the electrochromic performance. However, previous interpretations of the properties of these materials are not sufficiently clear to draw an unequivocal conclusion regarding their mechanism of fast ion diffusion. In this discussion we will review some of the previous experimental results and the models used to interpret them. We will show that in most cases the model that we propose can adequately account for all experimental observations.

For example, in WO_3 , it has been recognized²⁵ that crystalline samples have poor electrochromic properties that improve in polycrystalline films as the grain size is reduced. Thus, it has been speculated²⁵ that the good electrochromic properties are due to fast diffusion along the grain boundaries of crystalline grains, which themselves have low ionic conductivity. Experimentally, this model is not easily distinguishable from a model of a purely amorphous phase. Indeed, if crystalline grains of $\sim 25 \text{ \AA}$ are postulated, it is virtually impossible to distinguish this polycrystalline phase from an amorphous phase.

Our experiments on SIROF's show clearly that SIROF's are not polycrystalline on a very small scale (e.g., $\sim 25 \text{ \AA}$) but are indeed amorphous. The

proof of this lies in the DTA measurements, which show that a phase transition at $\sim 300^\circ\text{C}$ is associated with a very large release of energy (1.1 eV). It would be difficult to see why such a large release of energy should be associated with the increasing grain size of a polycrystalline film. Moreover, upon heating above $\sim 300^\circ\text{C}$ and up to 700°C , x-ray data show an increase in crystallite size, but the DTA does not indicate any measurable release of energy associated with grain growth. Thus a polycrystalline model similar to that postulated for WO_3 must be discarded in the case of the SIROF's.

Another electrochromic material that is similar to SIROF's is the anodically grown^{12,18} iridium oxide film (AIROF). These films show the same fast electrochromism and high catalytic activity of SIROF's but are much less stable. The bonding arrangement and stoichiometry of AIROF's have not been investigated in detail, and there is great confusion in the literature as to their structure. A fine-grain crystalline form of IrO_2 is used for modeling Faradaic processes.³³ Although recent experiments claim AIROF's to have an amorphous structure,²⁶ the only published experimental work reported that AIROF's have a hexagonal structure with a grain size $\sim 500 \text{ \AA}$.²⁷

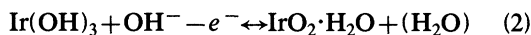
A proposed mechanism of electrochromism¹⁹ has been based on the insertion of protons into the channels of rutile IrO_2 . A mechanism based on hydroxide-ion insertion has been criticized²⁶ on the basis that hydroxide and other anions²⁸ are too large to enter the tetragonal rutile lattice. It is also reported that AIROF's are highly porous,^{26,27} and it is this high macroscopic porosity that has been consistently regarded as the main reason for the fast ion conduction and high catalytic activity.²⁰ On the other hand, SIROF's, which are not macroscopically porous (as shown by our SEM analysis and by recent electrocatalytic measurements²), have similarly good electrochromic and electrocatalytic properties. Thus, rather than the porosity, it is likely that the amorphous structure causes the good electrochromic and electrocatalytic properties of AIROF's.

A further point regarding the mechanism of electrochromism in AIROF's and SIROF's can be made from our experiments. The type and mechanism of ion insertion within these films is still unknown. In aqueous electrolytes two mechanisms have been proposed: (a) cation mechanism requiring coloration via proton extraction and (b) an anion mechanism requiring coloration

tion via hydroxide-ion insertion. Several experiments have supported one or the other mechanism. Recently, a careful analysis²⁹ (by Rutherford back-scattering and nuclear reaction techniques) has been employed to measure the relative oxygen and hydrogen content of colored and bleached AIROF's. These results are consistent with the proton mechanism, as they indicate that the colored film contains less hydrogen than the bleached film, i.e., the coloration reaction proceeds as



However, it is important to point out that the distinction between this and the anion mechanism is difficult. Indeed, an equation equivalent to (1) but involving hydroxide-ion insertion can be written as



where (H₂O) indicates unbound interstitial water³⁰ within the AIROF. In both Eqs. (1) and (2) the bleached state is Ir(OH)₃, while the colored state is IrO₂·H₂O, irrespective of the mechanism of coloration. Since the only difference between Eqs. (1) and (2) is the presence or absence of unbound water (which can readily be removed in vacuum), the analysis of Ref. 29 is also consistent with Eq. (2). Moreover, our experiments have shown that the structure of electrochromic iridium oxide films is amorphous and, therefore, does not restrict fast transport of large ions, such as OH⁻, so that Eq. (2) cannot be ruled out on the basis of low OH⁻ mobility as it would occur, for example, in a rutile structure. Thus, it is likely that proton extraction or hydroxide-ion insertion can result in the same electrochromic effect as indicated by Eqs. (1) and (2).

We can also compare the properties of SIROF to anodic ruthenium oxide, which is also an electrochromic ion-insertion material. Anodically grown ruthenium oxide shows a lower overvoltage for the oxygen evolution reaction than SIROF's; however, the high rate of corrosion renders them impractical for commercial interests.³¹ Although again as for AIROF's ruthenium oxide is reported as being microcrystalline,³² experimental work has indicated that anodic ruthenium oxide is amorphous to x rays. An exothermic phase transition³⁴ at ~300°C transforms the material into a polycrystalline phase with an increase in overvoltage for the oxygen evo-

lution reaction (and a decrease in the rate of corrosion). It would thus appear that for ruthenium oxide also the amorphous phase is the good catalyst, whereas the polycrystalline phase has lower catalytic activity (but greater stability).

VI. CONCLUSIONS

The major conclusion of this paper is that the good electrochromic and electrocatalytic properties of SIROF's are due to their amorphous structure. The amorphous structure provides fast³⁵ reversible ion transport and insertion for two reasons. First, it provides a random network of channels, some of which are sufficiently large to permit easy access of ionic species into the bulk of the material. Second, it provides empty ligand or vacant sites that provide the ionic species with temporary bonding sites. These channels and vacant sites do not necessarily result in a mechanically unstable structure. Like any glassy material the amorphous phase does contain a large number of strong bonds among randomly oriented molecules. Clearly, macroscopic porosity also favors ion insertion, but it is not essential when an amorphous structure is formed. On the other hand, porosity may have an adverse factor on stability. The porosity of the AIROF's is a possible source of their corrosiveness at high anodic voltages.

It is conceivable that other metal oxides may show fast ion insertion and transport when produced by reactive sputtering. For fast electrochromism, the metal oxide must have a sufficiently high electronic and ionic conductivity. We have seen that the amorphous phase of the SIROF formed by sputtering has a high ionic conductivity and an electronic conductivity, which, though significantly reduced with respect to the bulk phase, is still large enough to balance the enhanced ionic conductivity.

ACKNOWLEDGMENTS

We are grateful to our colleagues P. K. Gallagher (who collaborated with us in the early stages of this research³⁶), W. C. Dautremont-Smith, A. M. Glass, A. A. Pritchard, L. M. Schiavone, B. S. Schneider, and J. L. Shay for many useful contributions.

- ¹G. Beni, L. M. Schiavone, J. L. Shay, W. C. Dautremont-Smith, and B. S. Schneider, *Nature (London)* **282**, 281 (1979).
- ²S. Hackwood, L. M. Schiavone, W. C. Dautremont-Smith, and G. Beni, *Ext. Abstr. Electrochem. Soc.* **81-2**, 1262 (1981); *J. Electrochem. Soc.* **128-02**, 2569 (1981).
- ³L. M. Schiavone, W. C. Dautremont-Smith, G. Beni, and J. L. Shay, *Appl. Phys. Lett.* **35**, 823 (1979).
- ⁴L. M. Schiavone, W. C. Dautremont-Smith, G. Beni, and J. L. Shay, *Ext. Abstr. Electrochem. Soc.* **80-2**, 1299 (1980); *J. Electrochem. Soc.* **128**, 1339 (1981).
- ⁵G. Beni, *Solid State Ionics* **2**, 25 (1981).
- ⁶G. Beni and L. M. Schiavone, *Appl. Phys. Lett.* **38**, 593 (1981).
- ⁷S. Hackwood, W. C. Dautremont-Smith, G. Beni, L. M. Schiavone, and J. L. Shay, *J. Electrochem. Soc.* **128**, 1212 (1981).
- ⁸K. J. Vetter, *Electrochemical Kinetics* (Academic, New York, 1967).
- ⁹See, e.g., J. G. Posa, *Electronics* **53**, 39 (1980).
- ¹⁰G. G. Barna (private communication).
- ¹¹For general reference on displays see, e.g., *International Symposium, Digest of Technical Papers, Vol. XII* (Society for Technical Displays, New York, 1981).
- ¹²G. Beni and J. L. Shay in *Advances in Image Pick-Up and Displays*, edited by K. Kazan (Academic, New York, 1981).
- ¹³See, e.g., B. W. Faughwan and R. S. Crandall, in *Topics in Applied Physics*, edited by J. Pankove (Springer, New York, 1980), Vol. 40, p. 182.
- ¹⁴S. Hackwood, G. Beni, W. C. Dautremont-Smith, L. M. Schiavone, and J. L. Shay, *Appl. Phys. Lett.* **37**, 965 (1980).
- ¹⁵D. W. Murphy, F. J. DiSalvo, J. M. Carides, and J. V. Waszczak, *Mater. Res. Bull.* **13**, 1395 (1978).
- ¹⁶See, e.g., *Electrode Materials and Processes for Energy Conversion and Storage*, edited by J. D. E. McIntyre, S. Srinivasan, and S. J. Will (Electrochemical Society, Pennington, New Jersey, 1977).
- ¹⁷J. Horkans and M. W. Shafer, *J. Electrochem. Soc.* **124**, 1202 (1977).
- ¹⁸S. Gottesfeld, J. D. E. McIntyre, G. Beni, and J. L. Shay, *Appl. Phys. Lett.* **33**, 208 (1978).
- ¹⁹S. Gottesfeld and J. D. E. McIntyre, *J. Electrochem. Soc.* **126**, 742 (1979).
- ²⁰See, e.g., S. Gottesfeld and S. J. Srinivasan, *J. Electroanal. Chem.* **84**, 117 (1977).
- ²¹P. K. Gallagher, *Thermochim. Acta.* **26**, 175 (1978).
- ²²J. W. Mellor, *A Comprehensive Treatise on Inorganic and Theoretical Chemistry* (Longmans, Green and Co., London, 1953).
- ²³Cyclic voltammetry is a standard technique for studying electrochemical reactions in which the potential of the electrode is changed with time in a triangular wave form. The current is measured throughout the cycle and is plotted against the instantaneous potential. This current voltage plot is called a voltammogram. See, e.g., J. O'M. Bockris and A. K. N. Reddy, *Modern Electrochemistry* (Plenum, New York, 1970).
- ²⁴W. D. Ryden and A. W. Lawson, *Phys. Lett.* **26A**, 209 (1968).
- ²⁵K. S. Kang, PhD. thesis, London University, 1979 (unpublished).
- ²⁶J. D. E. McIntyre, W. F. Peck, Jr., and S. Nakahara, *J. Electrochem. Soc.* **127**, 1264 (1980).
- ²⁷D. Michell, D. A. J. Rand, and R. Woods, *J. Electroanal. Chem.* **84**, 117 (1977).
- ²⁸G. Beni, C. E. Rice, and J. L. Shay, *J. Electrochem. Soc.* **127**, 1342 (1980).
- ²⁹J. D. E. McIntyre, W. L. Brown, W. F. Peck, Jr., and W. M. Augustyniak (unpublished).
- ³⁰The interstitial unbound water could be partly responsible for the volume increase in the colored state. See S. Hackwood, W. C. Dautremont-Smith, G. Beni, L. M. Schiavone, and J. L. Shay, *J. Electrochem. Soc.* **128(b)**, 1212 (1981), and G. Gottesfeld and S. Srinivasan, *J. Electroanal. Chem. and Interfacial Electrochem.* **86**, 329 (1977).
- ³¹C. Iwakura, K. Hirao, and H. Tamura, *Electrochem. Acta* **22**, 329 (1977).
- ³²S. Gottesfeld, J. Rishpon, and S. Srinivasan (unpublished).
- ³³S. Gottesfeld, *J. Electrochem. Soc.* **127**, 1922 (1980).
- ³⁴C. Iwakura, K. Hirao, and H. Tamura, *Electrochem. Acta* **22**, 335 (1977).
- ³⁵Fast ion transport in the amorphous rather than in the polycrystalline phase has been observed in a wide variety of rapidly quenched glasses. See, e.g., A. M. Glass, K. Nassau, and D. H. Olson, in *Fast Ion Transport in Solids*, edited by P. Vashishta, J. N. Mundy, and G. K. Shenoy (North-Holland, Amsterdam, 1979), p. 707.
- ³⁶S. Hackwood, P. K. Gallagher, and G. Beni, *Solid State Ionics* **2**, 297, (1981).